

# A Dynamic Kick for the Nao Robot

Inge Becht  
Maarten de Jonge  
Richard Pronk

University of Amsterdam

June 5, 2013

## 1 Introduction

Our research is concerned with making a dynamic, closed loop, stabilized kick for the Nao robot. The Nao is a humanoid robot made by Aldebaran Robotics<sup>1</sup>. It is used in the Standard Platform League of the RoboCup<sup>2</sup>, an organization which organizes football (soccer) competitions for autonomous robots.

Kicking, of course, is an important part of football, and thus a good kick is vital to achieving good results in the RoboCup. There are essentially two ways of making a humanoid robot kick a ball:

1. Positioning the robot in a specific place relative to the ball, then executing a manually specified series of movements to kick the ball
2. Using the location of the ball and the direction you want the ball to go to dynamically determine a trajectory for the robot to follow

The first one is referred to as a *keyframe motion*, while the second one is the subject of this paper. In addition to just making a dynamic kick which only balances its own trajectory, it was also attempt to negate external forces from other robots.

## 2 Related Works

Seeing as the Nao robots were introduced to the Standard Platform League (SPL) of the RoboCup in 2007, this of course is not the first attempt at making a kicking motion for them. Notable publications in this area by other SPL teams include team B-Human ([8]) and Nao Team Humboldt ([10]).

One possible approach to kick generation is through machine learning, as done by [6].

A related, and very common task in humanoid robotics, is the creation of a walking gait. This shares a number of important subproblems with the task of kicking; most notably, balancing and inverse kinematics. The B-Human

---

<sup>1</sup><http://www.aldebaran-robotics.com/en/>

<sup>2</sup>[http://wiki.robocup.org/wiki/Standard\\_Platform\\_League](http://wiki.robocup.org/wiki/Standard_Platform_League)

team released an important paper in 2009 featuring not only a walk, but also a complete analytical inverse kinematics solution ([4]). Further techniques for balancing are proposed by [9], [5] and [1].

### 3 Basic information about the Nao

The Nao is a 58 cm high humanoid robot with a total of 21 degrees of freedom developed by Aldebaran Robotics. The Nao is equipped with all kinds of hardware that can be used to solve our problem. Here we will discuss the most important elements of the Nao that are useful for understanding the report. All experiments have been conducted on a RoboCup Nao H21, version 3.3 and 4.0.

#### 3.1 Foot sensors

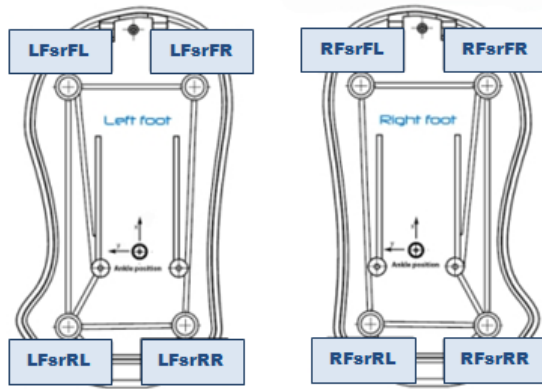


Figure 1: The force-sensitive resistors under Nao’s feet (courtesy of Aldebaran Robotics)

There are different hardware implementations for the Nao that can be used to figure out how stable it is in its current position. The one we use in this reports are the force-sensitive foot sensors. There are four of these sensors on either foot (as shown in Figure 3.1) which give a constant reading of the current pressure on each of the sensors.

#### 3.2 The coordinate space

Figure 3.2 shows the way in which the coordinate system works that we apply in our report. The x-axis point to the front of the Nao, while the y-axis points to the side and the z-axis upwards. All mentions of these axis in this report will be around this same coordinate frame.

## 4 Motivation for this project

While the Dutch Nao Team[3] (the team that represents the Netherlands in the Standard Platform League of the RoboCup) has achieved some degree of

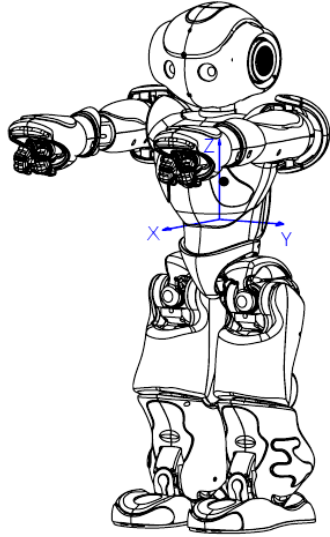


Figure 2: A schematic drawing of the Nao, showing his axis (courtesy of Aldebaran Robotics)

success with simple keyframe motions, they are clearly not optimal; a lot of time is wasted positioning the robot at just the right angle relative to kick the ball towards the goal. Furthermore, if the ball gets moved after the kicking motion has started, it is impossible for the robot to correct its kicking path. These are all problems that can be reduced with a dynamically generated motion, which is why we attempt to create one.

#### 4.1 Stability in a match

Since there is more than one player on the field chasing after the ball, lots of interference can be expected from pushing Naos while trying to perform a kick. Due to the instability of the Nao this results in falling down quite often, even more so when there is no compensation for it when executing a motion. A dynamic kick keeps track of how stable Naos current position is and compensates for outside disturbances while kicking.

#### 4.2 Harder kicks and better stability

Being able to define when a kick is stable enough to execute we can make a trade-off between how far the ball is kicked and the stableness of the robot, resulting in harder kicks then when using keyframe motions.

#### 4.3 Helping the Dutch Nao Team

Working on this project will help the Dutch Nao Team in their competition. The current keyframe motion used by DNT is very brittle. With our dynamic kick we create a more robust kick that can give our universities team a bigger chance of winning in competitions. This integration makes this project a valuable activity

in the long run, and not just a one time experiment that would not be further developed.

## 5 Methodology

The task of kicking a ball requires a couple of things: We need to plan a path for the foot to travel, then we need a way to calculate the joint angles corresponding to the required position of the foot (inverse kinematics), and all the while we have to make sure the robot doesn't fall over.

### 5.1 Automatic balancing during the kicking motion

The Nao should be balanced during its kick, regardless of the motion of the kicking leg. For this a center of mass-based approach ([10]) is used along with a proportional controller<sup>3</sup>.

#### 5.1.1 Center of mass and support polygon

This balancing approach requires knowledge of 2 concepts; the *center of mass*, and the *support polygon*. The center of mass (*CoM*) is the weighted average location of the Nao's mass, while the support polygon is the location on the floor over which the center of mass must be located to achieve stability. In the case of a robot standing on the ground, the support polygon is the convex hull of the feet touching the ground. Because the CoM is only used in conjunction with a proportional controller (which only requires a single target point) and the robot will only be balancing on one foot, the support polygon can be simplified to be a single point slightly in front of the location of the support leg's ankle joint.

The center of mass is defined as the sum of each component's *centroid* (its own center of mass) multiplied by its mass, divided by the total weight (equation 1). This of course requires each centroid to be described in the same coordinate system.

$$\frac{\sum_i \vec{c}_i m_i}{m} \quad (1)$$

In the Nao's documentation, each component's centroid is described relative to its own coordinate system, and offsets are included to convert between adjacent components coordinate systems. To handle this, we construct a chain of transformations to walk through each component recursively while calculating the center of mass of the entire robot.

#### 5.1.2 The proportional controller

The goal of the proportional controller (*P-controller*) is to keep the CoM as close as possible to the center of the support polygon at all times. The CoM is calculated relative to the standing leg's ankle joint, and we define the center of the support polygon to be "about 3 cm in front of that". Thus the error calculation becomes:

$$\begin{bmatrix} error_x \\ error_y \end{bmatrix} = \begin{bmatrix} 3 \\ 0 \end{bmatrix} - Co\vec{M}_{xy} \quad (2)$$

---

<sup>3</sup>[http://www.societyofrobots.com/programming\\_PID.shtml](http://www.societyofrobots.com/programming_PID.shtml)

The  $z$ -axis is ignored, because the height is irrelevant in this case (the CoM balancer only accounts for gravity, not other phenomena such as momentum).

The proportional control equation with two arbitrary *gain* parameters is shown in (3) and (4). The use of a different gain parameter for the  $x$ - and  $y$ -directions allows compensation for the fact that the Nao's feet (and really, feet in general) are rather elongated in the forward direction, making them far more stable to forces along the  $x$ -axis as opposed to the  $y$ -axis.

$$P_{out_x} = \text{gain}_x * \text{error}_x \quad (3)$$

$$P_{out_y} = \text{gain}_y * \text{error}_y \quad (4)$$

The value of  $P_{out_x}$  is inverted when balancing on the left leg because of the direction the joint rotates.

Actuation is achieved solely through the ankle's pitch and roll of the support leg. The rotation angles are obtained by searching through the set

$$\{(\theta_{pitch}, \theta_{roll}) \mid \theta_{pitch} \in \{0, P_{out_x}\}, \theta_{roll} \in \{0, P_{out_y}\}\}$$

and selecting the pair of angles with the largest reduction in error. This avoids situations where both components of the actuation interfere with each other and actually make the robot more unstable. This approach is acceptably fast when actuating two joints, but has the downside of having a complexity of  $\mathcal{O}(2^n)$  in amount of actuated joints.

## 5.2 Using force-sensitive resistors to keep balance

Although the CoM-based balancing allows for good convergence to a stable position, it does not react to external influences. Using the force-sensitive resistors under Nao's feet, these external influences can be measured and neutralized.

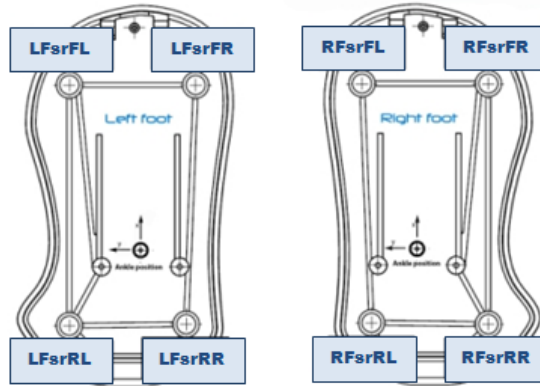


Figure 3: The force-sensitive resistors

The foot of the support leg will be divided into four sections (Front, Left, Right and Back).

- $Front_t = (1 - s) * Front_{t-1} + s * (LFsrl + LFsrr + RFsrl + RFsrr)$

- $Left_t = (1 - s) * Left_{t-1} + s * (LFsrFL + LFsrRL)$
- $Right_t = (1 - s) * Right_{t-1} + s * (LFsrFR + LFsrRR)$
- $Back_t = (1 - s) * Back_{t-1} + s * (LFsrRL + LFsrRR)$

Where  $s$  is the smoothing parameter and  $t$  is the present time.

### 5.2.1 Proportional-Derivative controller

The Proportional-Derivative controller (PD-controller) is a special case of the Proportional-Integral-Derivative controller (PID controller) where the integral term (I) is not used. The PD-controller has 2 terms, the proportional (P) and the derivative (D) term. The response of each term can be tweaked using their own tweaking parameter, the proportional gain  $K_p$  and the derivative gain  $K_d$ . The proportional term is given by:

$$P_{out} = K_p e(t)$$

and the derivative term is given by:

$$D_{out} = K_d \frac{d}{dt} e(t)$$

The hip pitch is used to compensate for the error in the  $x$  direction (*Front* and *Back*) while the hip roll compensates for the error in the  $y$  direction (*Right* and *Left*). The angle offsets for the hip joints are calculated by

- $e(t)_x = (Front_t - Back_t)$
- $e(t)_y = (Right_t - Left_t)$
- $P_{out}x = e(t)_x K_p$
- $P_{out}y = e(t)_y K_p$
- $D_{out}x = \frac{e(t)_x - e(t-1)_x}{timeTaken} K_d$
- $D_{out}y = \frac{e(t)_y - e(t-1)_y}{timeTaken} K_d$
- $Offset\ Hip\ Pitch = P_{out}x + D_{out}x$
- $Offset\ Hip\ Roll = P_{out}y + D_{out}y$

Where  $timeTaken = time_t - time_{t-1}$  (the time taken between the current and previous execution).

Using an error band allows for a range of stable points and therefore better convergence. Without this range the robot would diverge and finally fall due to oscillation. When the error is within this range it will be set to 0, this allows the robot to converge to a stable position. Due to the robot's build the forward and sideways stabilization act differently, different error bands are needed for either side. The function of the proportional term becomes:

$$P_{out}x = \begin{cases} e(t)_x K_p & \text{if } e(t)_x < Thres_{minX} \text{ or } e(t)_x > Thres_{maxX} \\ 0 & \text{Otherwise} \end{cases}$$

$$P_{outy} = \begin{cases} e(t)_y K_p & \text{if } e(t)_y < Thres_{minY} \text{ or } e(t)_y > Thres_{maxY} \\ 0 & \text{Otherwise} \end{cases}$$

Where  $Thres_{min}$  is the lower bound of the error band,  $Thres_{max}$  is the upper bound and  $K_p$  is the first tweak parameter of the PD-controller.

$Thres_{minX} = -Thres_{maxX}$  and  $Thres_{minY} = -Thres_{maxY}$ .

$$D_{outx} = \begin{cases} \frac{e(t)_x - e(t-1)_x}{timeTaken} K_d & \text{if } e(t)_x < Thres_{minX} \text{ or } e(t)_x > Thres_{maxX} \\ 0 & \text{Otherwise} \end{cases}$$

$$D_{outy} = \begin{cases} \frac{e(t)_y - e(t-1)_y}{timeTaken} K_d & \text{if } e(t)_y < Thres_{minY} \text{ or } e(t)_y > Thres_{maxY} \\ 0 & \text{Otherwise} \end{cases}$$

### 5.2.2 Sampling Rate Issues

Using the balancer as it is now requires different parameters for every sampling rate. Since the sampling rate is determined by the available CPU power, a fix is needed that will add the sampling rate in the calculation. Doing this allows the same parameters to be used regardless of the background processes or CPU type. The following fix is applied:

- $Offset\ Hip\ Pitch = (P_{outx} + D_{outx}) * timeTaken$
- $Offset\ Hip\ Roll = (P_{outy} + D_{outy}) * timeTaken$

With this fix the angle offsets will be relative to  $timeTaken$ , giving a bigger offset when the time between the executions is larger and vice versa. This gives us a timing-independent compensation architecture which adapts to the available CPU power.

### 5.2.3 The setup error

As the script runs the first measurements of  $timeTaken$  are relatively big in some cases even a factor 100 from the normal value. This big value will change the angles in such a way that the robot will overshoot and possibly even fall. Therefore disregarding these values will be necessary, adding a low-pass filter to  $\Delta timeTaken$  allows finding these measurements. When the threshold of the low-pass filter has been exceeded the angle offsets will be set to 0, ignoring the large values.

$$Offset\ Hip\ Pitch = \begin{cases} (P_{outx} + D_{outx}) * timeTaken & \text{if } \Delta timeTaken < Thres_{low-pass} \\ 0 & \text{Otherwise} \end{cases}$$

$$Offset\ Hip\ Roll = \begin{cases} (P_{outy} + D_{outy}) * timeTaken & \text{if } \Delta timeTaken < Thres_{low-pass} \\ 0 & \text{Otherwise} \end{cases}$$

Where  $Thres_{low-pass}$  is the threshold value for the low-pass filter.

## 5.3 The kinematics problem

We want to be able to specify a location for the foot, then have the foot automatically move there, which means that we'll need to be able to calculate the required joint angles. This is known as *inverse kinematics*. There is a number of potential solutions to this problem, for example:

- analytically solve the inverse kinematics chain using goniometry (as done by [4])
- use an iterative algorithm to approach the desired location over a number of iterations ([2])

We wound up going with an iterative, Jacobian-based solution as decribed by [7] and [2]. To see a short summary of other experimentations, see appendix A.

### 5.3.1 Problem specification and terminology

Let:

- $\theta$  be a  $1 \times n$  vector describing the angles of  $n$  joints ( $\theta = [\theta_1 \dots \theta_n]^T$ )
- $\vec{t}$  the vector containing the goal position for each end effector
- $\vec{s}$  the vector of the end effectors' current positions

$\vec{t}$  and  $\vec{s}$  are both of size  $1 \times f$  where  $f$  is the desired amount of degrees of freedom in the end effectors (generally 3 if you only care about the spatial location, or 6 if you take the rotation into account too). Thus, if you have  $k$  end effectors and 3 degrees of freedom in your position:

$$\begin{aligned}\vec{t} &= [t_1, \dots, t_k]^T \\ \vec{s} &= [s_1, \dots, s_k]^T\end{aligned}$$

where

$$\begin{aligned}t_i &= [t_{i_x}, t_{i_y}, t_{i_z}]^T \\ s_i &= [s_{i_x}, s_{i_y}, s_{i_z}]^T\end{aligned}$$

Viewing the end effectors locations as a function of the joint angles, we want to find values for  $\theta$  such that  $\vec{t} = \vec{s}(\theta)$ . One way to do this is by taking a linear approximation of the function with respect to the joint angles, and slightly adjusting the angles to get closer to the solution. Over a number of iterations, the end effectors will hopefully converge to the desired position. This linear approximation is done using the Jacobian matrix  $J$ , defined as:

$$J(\theta)_{i,j} = \frac{\partial s_i}{\partial \theta_j} \quad (5)$$

$$\frac{\partial s_i}{\partial \theta_j} = v_j \times (s_i - p_j) \quad (6)$$

In the case of a rotational joint (as is the case with every joint on the Nao robot), the the entries of the Jacobian are given by (6), where  $v_j$  is a unit vector describing the axis of rotation of the joint belonging to  $\theta_j$  and  $p_j$  is the location of that joint in space.

Using the Jacobian matrix, the change in end effector locations corresponding with a certain change in joints angles can be described as:

$$\Delta \vec{s} \approx J \Delta \theta$$

$\Delta\vec{s}$  should be as close as possible to the error  $\vec{e} = \vec{t} - \vec{s}$ , which means that the equation we're looking for is:

$$\Delta\theta = J^{-1}\vec{e}$$

Since the Jacobian will generally not be invertable, its inverse will have to be approximated. Some methods of approximation include the Jacobian transpose method, the Moore-Penrose pseudo-inverse, and the Levenberg-Marquardt damped least squares method (see [2]).

### 5.3.2 The algorithm

We opted to go for a 3-dimensional positioning, without regards for the rotation of the end-effector (see section 5.4 for motivation). Because the ankle joint is taken as end-effector, the ankle itself has no influence on the location. This leaves us with 4 joints; the pitch, roll and yaw of the hip, along with the knee's pitch.

Because the Jacobian only gives a linear approximation, the joints tend to behave erratically when a target location is far away. This is counteracted by moving the target closer if the distance exceeds a certain threshold. This is done according to (7).

$$\vec{e} = \begin{cases} \vec{t} - \vec{s} & \text{if } \|\vec{t} - \vec{s}\| < D_{max} \\ D_{max} \frac{\vec{t} - \vec{s}}{\|\vec{t} - \vec{s}\|} & \text{otherwise} \end{cases} \quad (7)$$

Pseudocode for the entire algorithm can be seen in algorithm 1.

When updating the joint angles ( $\theta$ ), take care to restrict them to their actual range to avoid a solution with impossible angles.

## 5.4 The Kick

With the solutions to the previous aspects of the dynamic kick constructed, we can start to calculate the optimal kicking trajectory. This kick is composed of different stages, loosely based on the approach of [10].

- Initial pose
- Retraction point
- Contact point

For all these stages we assume we have knowledge about the coordinates of the ball in some coordinate system relative to the Nao or a fixed point in space, the size of the ball to hit and which way we want to kick the ball.

### 5.4.1 Initial pose

The first stage is the initial pose. The Nao positions its center of mass on top of its standing leg. This is done by setting the Nao in NormalPose (a keyframe motion made by the Dutch Nao Team) and turning on the CoM-balancer.

---

**Algorithm 1** The inverse kinematics solution

---

```
function INVERSE_KINEMATICS(target,  $\lambda$ , max_iter,  $D_{max}$ , threshold)
    best_error =  $\infty$ 
    best_theta = nil
     $\theta \leftarrow$  the current body angles
    while n_iter < max_iter do
         $\vec{s} \leftarrow$  the current end effector position
         $\vec{e} \leftarrow \text{target} - \vec{s}$ 
        error  $\leftarrow \|\vec{e}\|$ 
        if error < best_error then
            best_error  $\leftarrow \text{error}$ 
            best_theta  $\leftarrow \theta$ 
        end if
        if best_error < threshold then
            return best_theta
        else
             $J \leftarrow \text{get_jacobian}(\theta)$ 
            if  $\|\vec{e}\| > D_{max}$  then
                 $\vec{e} \leftarrow D_{max} \frac{\vec{e}}{\|\vec{e}\|}$ 
            end if
             $J^{-1} \leftarrow J^T (J J^T)^{-1} + \lambda^2 I(3)$        $\triangleright I(3)$  is the  $3 \times 3$  identity matrix
             $d\theta \leftarrow J^{-1} * \vec{e}$ 
             $\theta \leftarrow \theta + d\theta$ 
        end if
    end while
    return best_theta
end function
```

---

### 5.4.2 Contact point

The contact point is the point on the ball that has to be hit by the Nao to move it in the desired direction. [10] uses the following calculation to find this, which seems to work exactly as we would like:

$$\vec{c} - (\vec{e} * r)$$

where  $\vec{c}$  is the location of the center of mass of the ball,  $r$  is the ball radius (in the case of the SPL balls this is 33.42 mm) and  $\vec{e}$  is the force destination (the direction of where we want the ball to end up in coordinates).

### 5.4.3 Retraction point

After the initial pose the Nao calculates its optimal retraction point. This is the rearmost point from which the kick commences, and has two criteria that should be satisfied to be considered a good starting position:

- The retraction point should be far away from the ball (to make the kick as hard as possible)
- The retraction point should be accurate

To meet both criteria as good as possible there should be a trade off between the two.

Firstly, to determine the point between the ball and a possible retraction point we use the following calculation:

$$d_r = \vec{e}^x * ||\vec{p}^x - \vec{p}_c^x|| + \vec{e}^y * ||\vec{p}^y - \vec{p}_c^y|| + ||\vec{p}^z - \vec{p}_c^z|| * 0.3 \quad (8)$$

Where  $\vec{p}_c$  is the contact point where the ball should be hit,  $\vec{p}$  is a possible retraction point,  $\vec{e}$  is the unit vector pointing to the desired destination and  $d_r$  the distance between both points. The importance of the  $x$  and  $y$  distance between the contact point and a possible retraction point relies on how much of the unit vector points to that direction. The  $z$  is held artificially high so that the leg will never be stretched to the ground.

Finding the accuracy of a given retraction point is less straightforward. This problem can be seen as the closeness of a given point to the line, where the point consists of a possible retraction point and the line consists of the contact point and the destination point. See Figure 4 for a visualisation of the problem. This idea makes for a basic linear algebra<sup>4</sup> problem that needs to be resolved.

$$d_a = \frac{||(\vec{p}^{xy} - \vec{p}_c^{xy}) \times (\vec{p}^{xy} - \vec{f}_d^{xy})||}{\|\vec{f}_d^{xy} - \vec{p}_c^{xy}\|}$$

The distance to the line is only important in the  $xy$  direction, but a cross product can only be taken in 3D so this is solved by taking the  $xy$  values from the original points in space but adding a 0 value in the  $z$  direction. Now that we have a way to calculate both the distance to the contact point and the accuracy

---

<sup>4</sup>The intuition behind this calculation can be found on <http://mathworld.wolfram.com/Point-LineDistance3-Dimensional.html>

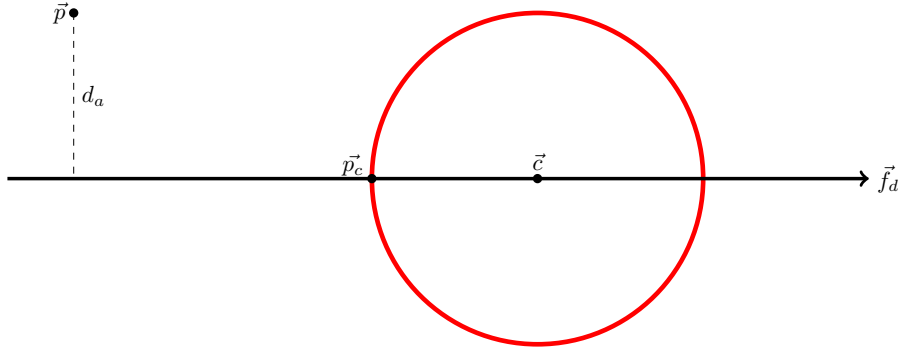


Figure 4: Visualisation of the accuracy problem. the contact point ( $\vec{p}_c$ ) and the preferable force direction ( $\vec{f}_d$ ) form a line in 3D space. A possible retraction point  $\vec{p}$  can be somewhere around this line. To find its accuracy the distance  $d_a$  should be solved. Note that this only concerns the x and y direction as the z dimension does not influence the accuracy.  $\vec{c}$  denotes the center of mass location on the ball and is only shown for clarification.

towards the force direction, we are able to make a balanced decision towards what a good retraction point is.

$$\vec{p} = (1 - \delta) * d_r + \delta * \frac{100}{d_a} \quad (9)$$

We take the multiplicative inverse of  $d_a$  so that the value gets bigger when the retraction point is close to the line and rescale it by multiplying it with 100 to make the value  $d_r$  and  $d_a$  more in the same range. The value  $\delta$  could be experimented with to find the optimal result. Accuracy is more important than a big distance between ball and retraction point, something that will become evident in the results section.

All possible positions  $\vec{p}$  should be considered to solve this equation. To determine what is possible the Nao is set in different positions and using a forward kinematics chain the end effector of each leg where the origin is the supporting foot can be retrieved. This way roughly all possible positions are set and can be looped through to find the point that maximizes above equation. By also retrieving the location of the standing leg we make sure that there is no overlap in the reachable space and the position of the other leg.

## 6 Experiments and Results

### 6.1 Using force sensitive resistors for balancing

Since balancing in the  $y$  direction is the biggest challenge to stabilize we used another Nao to push the balancing Nao in this direction (see Figure 5). We ran the script twice, one time with the balancer on and the second time where the offsets of the angles were forced to 0 (keeping the plotting function but killing the balance system)

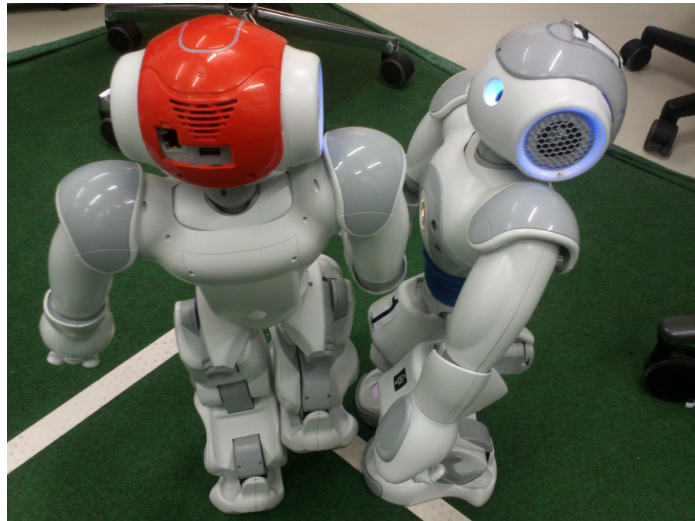


Figure 5: Nao (right) pushing the other Nao (left) in the sideways (y) direction

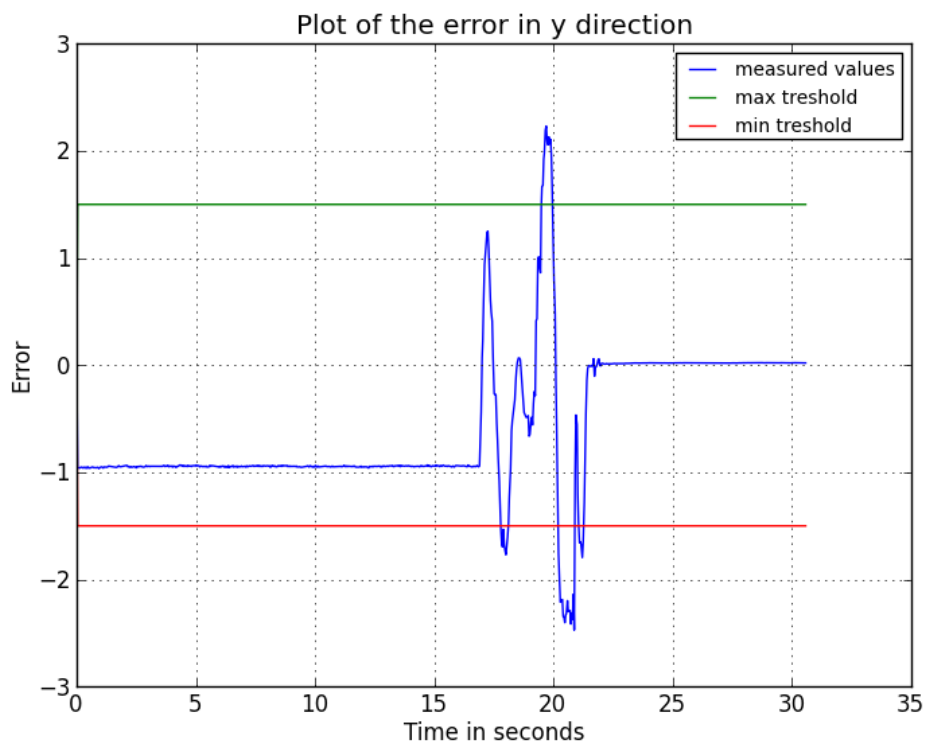


Figure 6: With the balancer turned off (The Nao falls at 22 seconds)

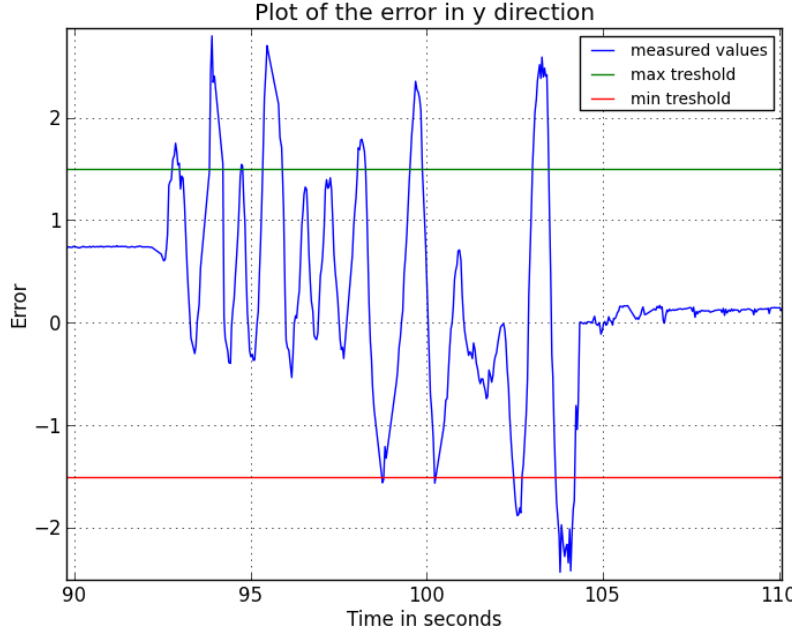


Figure 7: With the balancer turned on (The Nao falls at 104 seconds)

As seen in the plots (Figure 6 and Figure 7), using the balancer helps to stay up longer (twice as long) but still can't fully handle the external influences from the pushing Nao. The problem is that there aren't many stable poses in the sideways direction and even a small change will have a relative large influence on the sensor data. Due to this the sideways balancing tends to overshoot and then start to oscillate. Taking a low  $K_p$  and  $K_d$  values gives a long settling time but minimizes the overshoot. The system now converges relative slow to a stable position but is still able to negate external influences, providing a more stable and reliable balancer.

## 6.2 Inverse kinematics

Since our inverse kinematics solution relies on two parameters ( $\lambda$  and  $D_{max}$ , see section 5.3), some testing needs to be done to optimize these. For testing, 3 reasonable target positions were chosen, where the parameters were chosen from the set  $\{\lambda, D_{max} \mid \lambda \in (0.1, 0.25, 0.5, 1, 5), D_{max} \in (10, 20, 30, 40, 50)\}$ . The results can be seen in figures 8, 9 and 10. The error in the plots is defined as  $\|\vec{t} - \vec{s}\|$ . Due to the large number of colored squiggly lines, each plot has been restricted to only parameter combinations which converged relatively quickly to aid in readability.

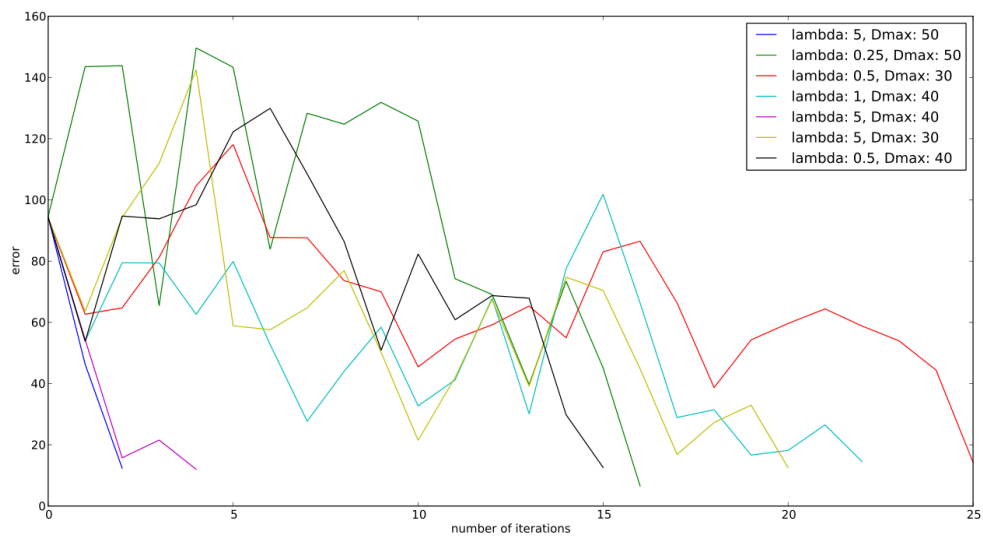


Figure 8: The first position, with the positional error set out against the time.

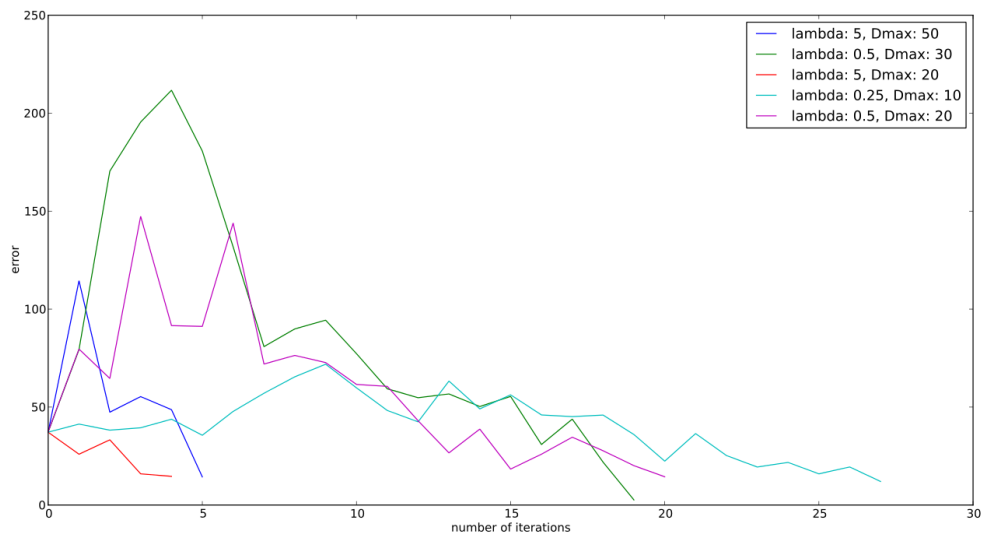


Figure 9: The second position, with the positional error set out against the time.

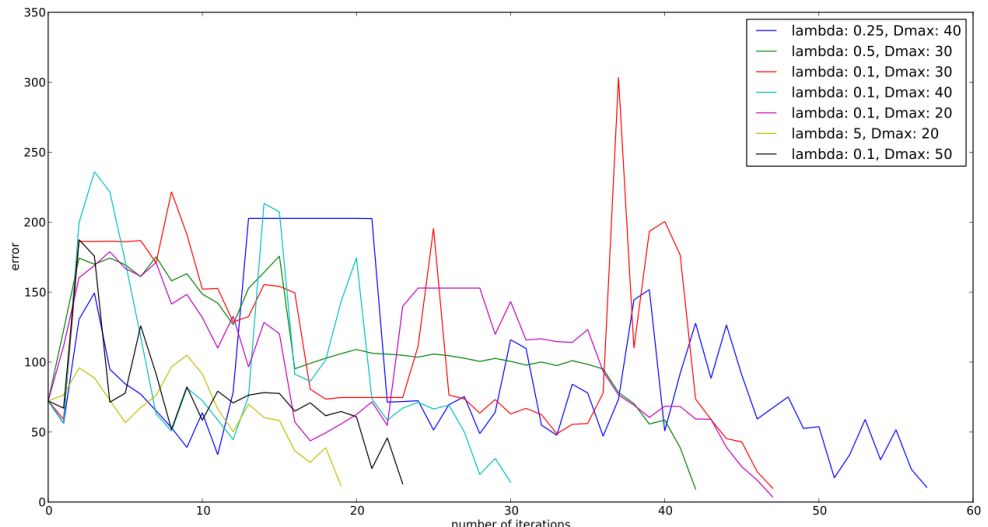


Figure 10: The third position, with the positional error set out against the time.

In each case, the optimal value for  $\lambda$  was 5, while  $D_{max}$  was either 50 or 20, which is a relatively large difference given the range of values. Of course, three tests isn't enough to conclusively determine the optimal parameters, but they offer a nice starting point for further practical testing.

### 6.3 Calculating the retraction point

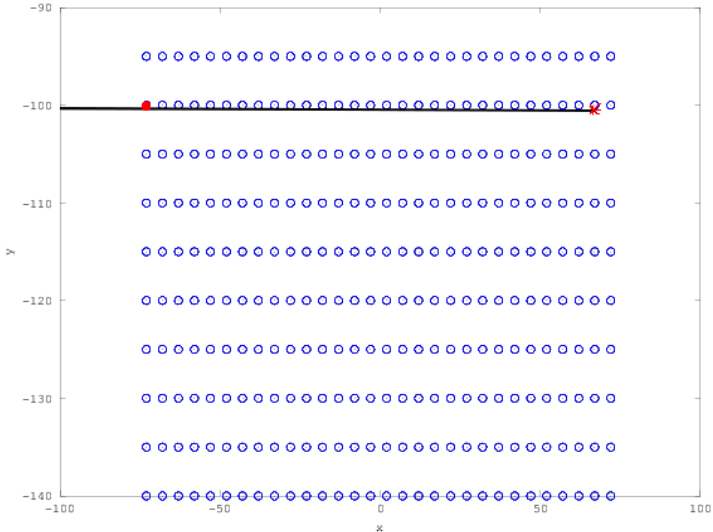


Figure 11: Visualisation of relevance of all tried retraction points. The red point is the finally used point. The red asterisk is the contact point. In this case the ball should be kicked straight forward.

To see how well the calculation of the retraction point really works, we visualised the different points that were tried out. Figure 11 is the result of a direction  $[1 \ 0 \ 0]^T$  and a center of mass positioning of the ball right in front of the right foot (the kick commenced with the right leg as well). The line is the point on which we would like to see the foot retraction take place, as it is the line on which both the direction and the contact point of the ball lie. The blue dots are the reachable positions that are evaluated as possible retraction points. The red dot is the chosen retraction point the Nao executes, and the red asterisk is the contact point. For this experiment we chose  $\delta = 0.999$  in equation 9, so that accuracy was more important than distance. The effect is in this case that still the point with the greatest distance is chosen because the whole row of those points have the same accuracy so still the one with the biggest distance to the contact point gets chosen.

Another experiment shows the same idea but, instead of kicking straight ahead, the direction was with an angle to the left, more precise with  $\vec{e} = \left[ \frac{1}{\sqrt{2}} \ \frac{1}{\sqrt{2}} \ 0 \right]^T$ . Using the same  $\delta$  value as before gave us the result as can be seen in figure 12. It is the most accurate point given a list of possible elements.

Although there is another good point (at approximate (-60, -140)) it is nearly impossible to get this value as the chosen optimal point. When lowering the  $\delta$  value even slightly it changes the distance drastically in the x direction, making the trade-off less pronounced than imagined.

Another visualisation can be seen in figure 13. In this case the ball should be kicked straight ahead again (direction =  $[1 \ 0 \ 0]^T$ ). All blue dots are evaluated retraction points and the red stars are the points that are the most

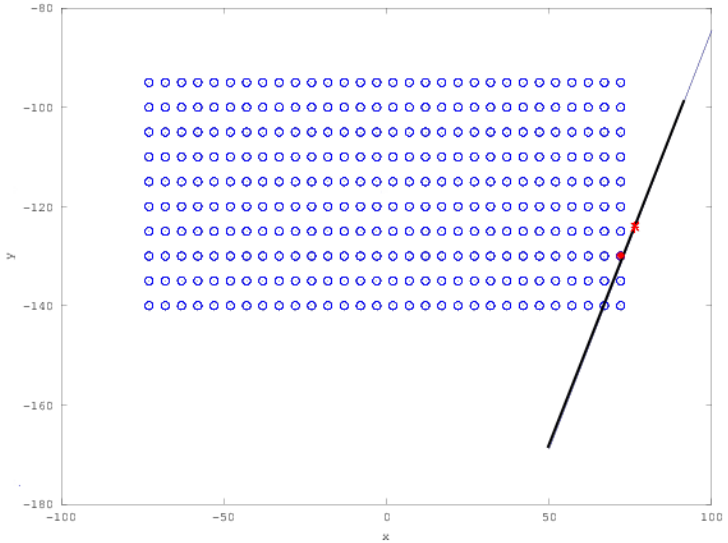


Figure 12: Visualisation of relevance of all tried retraction points. The red point is the finally used point, the red asterisk is the contact point. In this case the ball is kicked with an angle.

accurate(all have the same value). The data is set out over the  $xy$  axis, which is the added length of the  $x$  and  $y$  direction, the  $z$  axis and the *distance* is the distance as we measure it in 8 between contact point and the ball. The fact that sometimes multiple of the same  $xy$  and  $z$  combinations have different distances to the contact point is to be understood from the fact that although in the axis both the real value of  $x$  and  $y$  are added to each other, equation 8 only considers the value of  $x$  when the ball should go straight ahead.

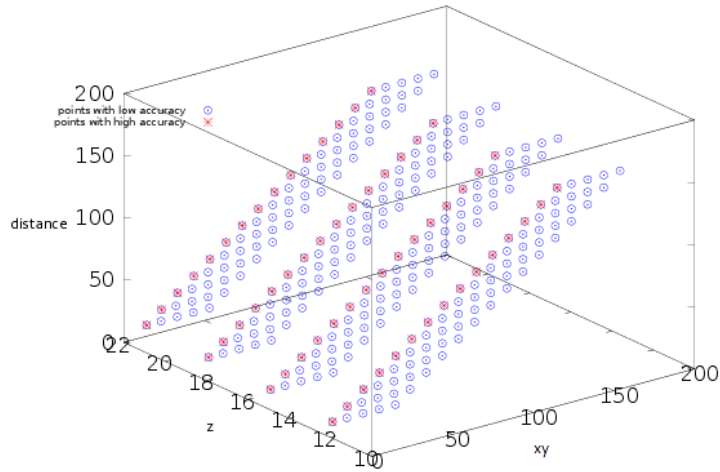


Figure 13: Plot where the length of the  $xy$  direction between the contact point and the retraction point are set out against the  $z$  direction and the  $distance$  from equation 8. The red points indicate the most accurate position

#### 6.4 Integration of the Center of Mass balancers with the kick

Because of the limited ranges of both legs when it comes to reaching a ball we would like the Nao to stand straight as much as possible while performing a kick. When executing the initial pose we use the CoM balancer to seek the most balanced position, but it makes a lot of difference as to which joints in the support leg are used for balance. At first we experimented with the *HipRoll* and *HipPitch* to move to the most stable position. This however made for quite an unnatural pose, as you can see in Figure 14(a). Because executing a kick only uses the kicking leg, it can reach less of the relevant places.

Using the angle of the *AnkleRoll* and *AnklePitch* in the initial pose delivers a more natural position as seen in Figure 14(b), which makes it a better decision for the initial pose.

## 7 Conclusion

Although the individual components mostly work as planned, integrating them all into an actual kick has proven harder than expected, which has left us unable to test the interactions between all of the components. For instance, using only the hip to compensate for balance is effective in the sense that it's good at balancing, but it results in poses where the kicking leg is unable to reach even near the ground. Using the ankle however works just as well for balance, and doesn't suffer from the same problem. Unfortunately, there was no time for further testing in this regard.

Generation of the kick trajectory appears to work properly, although it hasn't been thoroughly tested (only in a few directions) due to time constraints. Similarly, there is no data regarding the strength or stability of the kick, simply because there is no final kick yet.

The balancing system seems to work quite well and has been quite vigorously tested. Still interferences from the side stay problematic, but only playing a real math with the balancing turned on will show if it will work decent enough.

In the end, we've ended up with a nice motion framework which needs a bit more work in order to have a completely functioning kick, which will hopefully function as a basis for further motion-related tasks for the Dutch Nao Team (such as a new walking motion).

## 7.1 The retractionpoint

The above experimentations with finding a retractionpoint while making a trade-off between accuracy and distance seems to conclude that the retraction calculation works as was expected for the basic cases. Due to time constraints, and the fact that less straightforward kicks are hard to visualise on a graph there are still cases left out, but it already makes for a successful kick in the most basic of situations.

# 8 Future works

Now that all subproblems of making a dynamic kick seem to be solved successfully, there are still some future improvements we would like to work on.

## 8.1 Wrapping up our current work

Firstly, we would like to integrate all elements talked about to make a successful kick. This was something we wanted to complete by the time this project ended, but in hindsight was a little too advanced for the limited timeframe. Nevertheless, we were still able to find solutions to every problem and can take our time to combine both controllers and the kicking motion into a worthy final result.

## 8.2 Porting everything to C++

Many components were written in Python to aid in rapid prototyping, with help from the Numpy module to allow for acceptable speeds. This works decently, but we unfortunately don't have a way of running Numpy on our robots. Seeing as the Dutch Nao Team plans on switching to C++ for their codebase in the near future, porting everything to C++ seems like the best option.

# A Experimentations with solving the inverse kinematics problem.

Before we arrived at our final inverse kinematics solution, we tried a number of different (seemingly easier) options first. This section details some of these experimentations and why we have abandoned them.

## A.1 Using built-in functions

The Naoqi framework running on the Nao robots offers a *Cartesian Control API*<sup>5</sup> which contains a number of inverse kinematics function for setting and requesting end effector locations in a specified coordinate system. The possible coordinate systems were “world” (where the origin was somewhere arbitrarily around the Nao), the torso and one between the legs. Because both the torso coordinate system and the one between the legs are dependent of the posture of the Nao, we tried to work with the coordinate somewhere in space. To determine the range of the legs we took the Nao by hand and set the legs in the most stretched positions and retrieved the maximum and minimum  $x$ ,  $y$  and  $z$  values. These were taken as absolute ranges relative to a starting position. In the end this approach didn’t work as making a request for the current position as well as setting a new position in this coordinate frame was not reliable enough. It seemed that the sensor values used to find these positions weren’t well enough to use for such an operation. Another big problem is that actuation appeared to be quite slow; far too slow for a powerful football kick.

## A.2 Using a simulator to find all reachable positions

We also tried to use the Cartesian Control API in a simulated environment<sup>6</sup> to obtain a table containing all reachable locations of a given leg, within a certain resolution. Throughout a given range of world positions, the Nao was made to move its foot there, after which the position of the foot was requested to see if the position had been reaches. In the end this was not as reliable as hoped due to the same issues as spoken in the last section.

## A.3 Making a lookup-table using Forward Kinematics

Because we already had a workable solution for forward kinematics, we thought about creating a lookup table by iterating through a collection of joint angles and saving them in a hashmap along with the corresponding end effector position. Integrating this using the balancing system however became a bit harder because we needed to track the position of the hip angles (these were, at the time used for changing the pose of the Nao) in the support leg, and in the end constructing the inverse kinematics ourselves was an easier solution.

## References

- [1] JJ Alcaraz-Jiménez, M Missura, H Martinez-Barbera, and S Behnke. Lateral Disturbance Rejection for the Nao Robot. *Proceedings of the 16th RoboCup Symposium, Mexico, June 2012*, 2012.
- [2] Samuel R Buss. Introduction to Inverse Kinematics with Jacobian Transpose , Pseudoinverse and Damped Least Squares methods. <http://math.ucsd.edu/~sbuss/ResearchWeb/ikmethods/iksurvey.pdf>, 2009.

---

<sup>5</sup><http://www.aldebaran-robotics.com/documentation/naoqi/motion/control-cartesian.html>

<sup>6</sup>The environment used can be found on <http://www.nao.sandern.com>

- [3] Dutch Nao Team. Dutch Nao Team - Team Description for Robocup 2012 - Mexico City, Mexico. Technical report, 2012. to be published on the Proceedings CD of the 16th RoboCup Symposium, Mexico, June 2012.
- [4] Colin Graf, Alexander Härtl, Thomas Röfer, and Tim Laue. A Robust Closed-Loop Gait for the Standard Platform League Humanoid. *Proceedings of the Fourth Workshop on Humanoid Soccer Robots in conjunction with the 2009 IEEE-RAS International Conference on Humanoid Robots*, pages 30–37, 2009.
- [5] Colin Graf and Thomas Röfer. A closed-loop 3D-LIPM gait for the RoboCup Standard Platform League humanoid. *Fourth Workshop on Humanoid Soccer Robots in*, 2010.
- [6] Christiaan Meijer. Getting a kick out of humanoid robotics - Using reinforcement learning to shape a soccer kick. Master's thesis at the University of Amsterdam, 2012.
- [7] Michael Meredith and Steve Maddock. Real-time inverse kinematics: The return of the jacobian. Technical report, 2004. <http://www.dcs.shef.ac.uk/intranet/research/resmes/CS0406.pdf>.
- [8] Judith Müller, Tim Laue, and Thomas Röfer. Kicking a Ball Modeling Complex Dynamic Motions for Humanoid Robots. *RoboCup 2010: Robot Soccer World Cup XIV*, pages 109–120, 2011.
- [9] Johannes Strom and George Slavov. Omnidirectional walking using zmp and preview control for the nao humanoid robot. *RoboCup 2009: Robot Soccer World Cup*, pages 378–389, 2010.
- [10] Yuan Xu and Heinrich Mellmann. Adaptive motion control: Dynamic kick for a humanoid robot. *KI 2010: Advances in Artificial Intelligence*, pages 392–399, 2010.



(a) Using the *HipRoll* and *HipPitch* to balance the Nao



(b) Using the *AnklePitch* and *AnkleRoll* to balance the Nao

Figure 14: Experimentation with the influence of joint choice on the balancer